Supporting Information

Layered Boron–Nitrogen–Carbon–Oxygen Materials with Tunable Composition as Lithium-Ion Battery Anodes

Jonathan Tzadikov,[a] Mahmud Auinat,[b] Jesús Barrio,[a] Michael Volokh,[a] Guiming Peng,[a] Christel Gervais,[c] Yair Ein-Eli,[b] and Menny Shalom*[a]

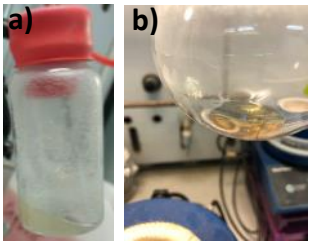

Figure S1. (a) image of the homogeneous liquid, which is formed above 150 °C for a mixture of borane-ammonia complex and pheananthrene., and (b) image of molten pyrene

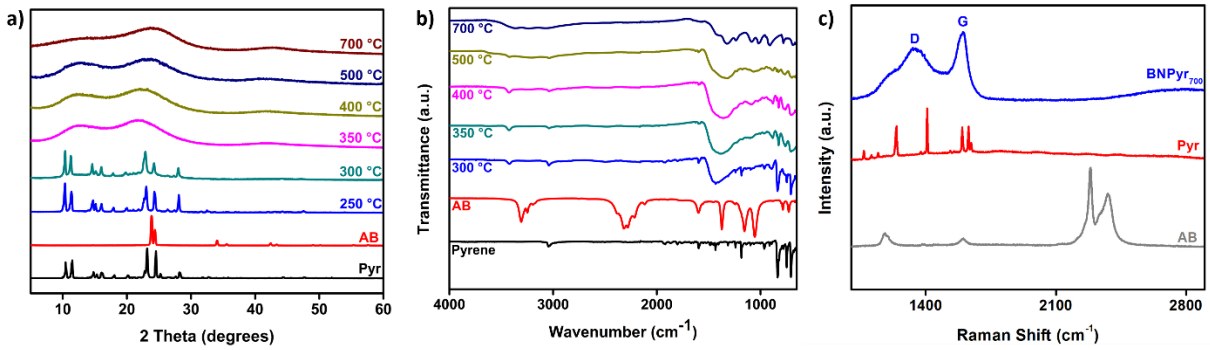

Figure S2. a) X-ray diffraction patterns of BNPyr$_{250, 300, 350, 400, 500, 700}$, Pyr, and AB; b) Fourier transform infra-red (FTIR) spectra of BNPyr$_{300, 350, 400, 500, 700}$, Pyr, and AB; c) BNPyr$_{700}$, Pyr, and AB Raman spectra. Patterns and spectras are offset for clarity.

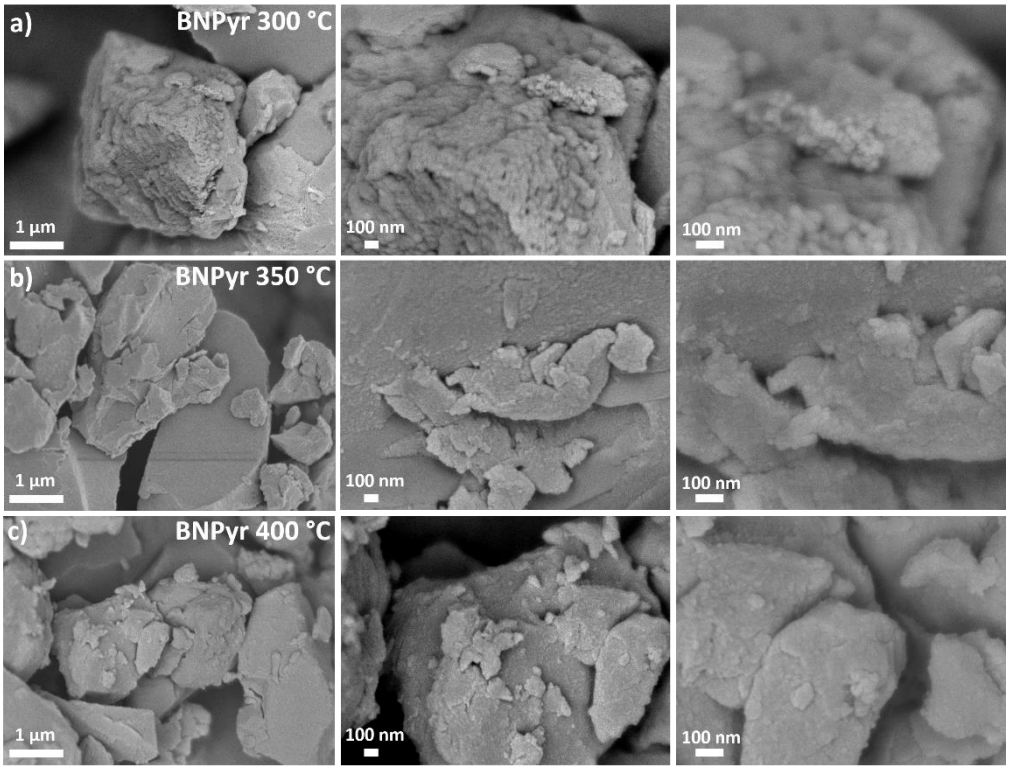

Figure S3. SEM images of a) BNPyr$_{300}$, b) BNPyr$_{350}$, and c) BNPyr$_{400}$.

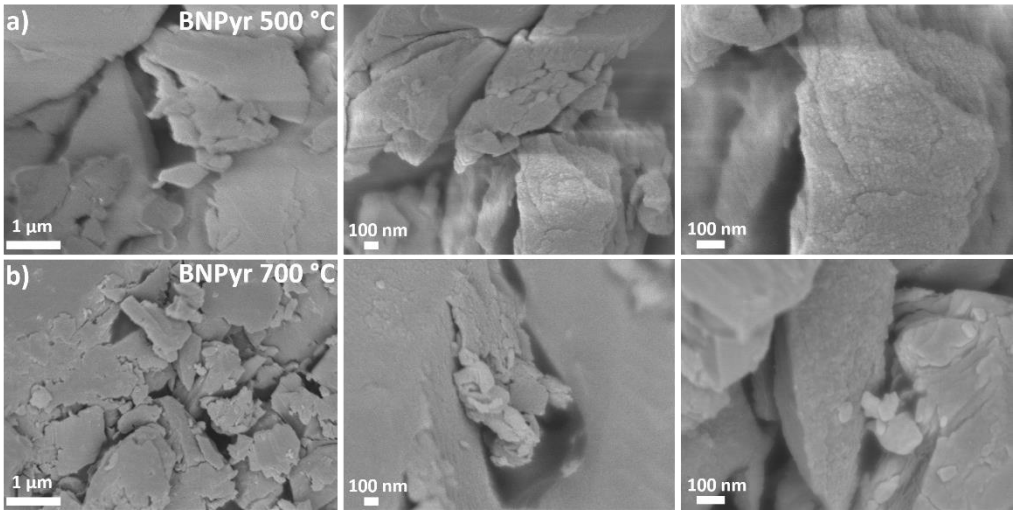

Figure S4. SEM images of a) $BNPyr_{500}$, b) $BNPyr_{700}$.

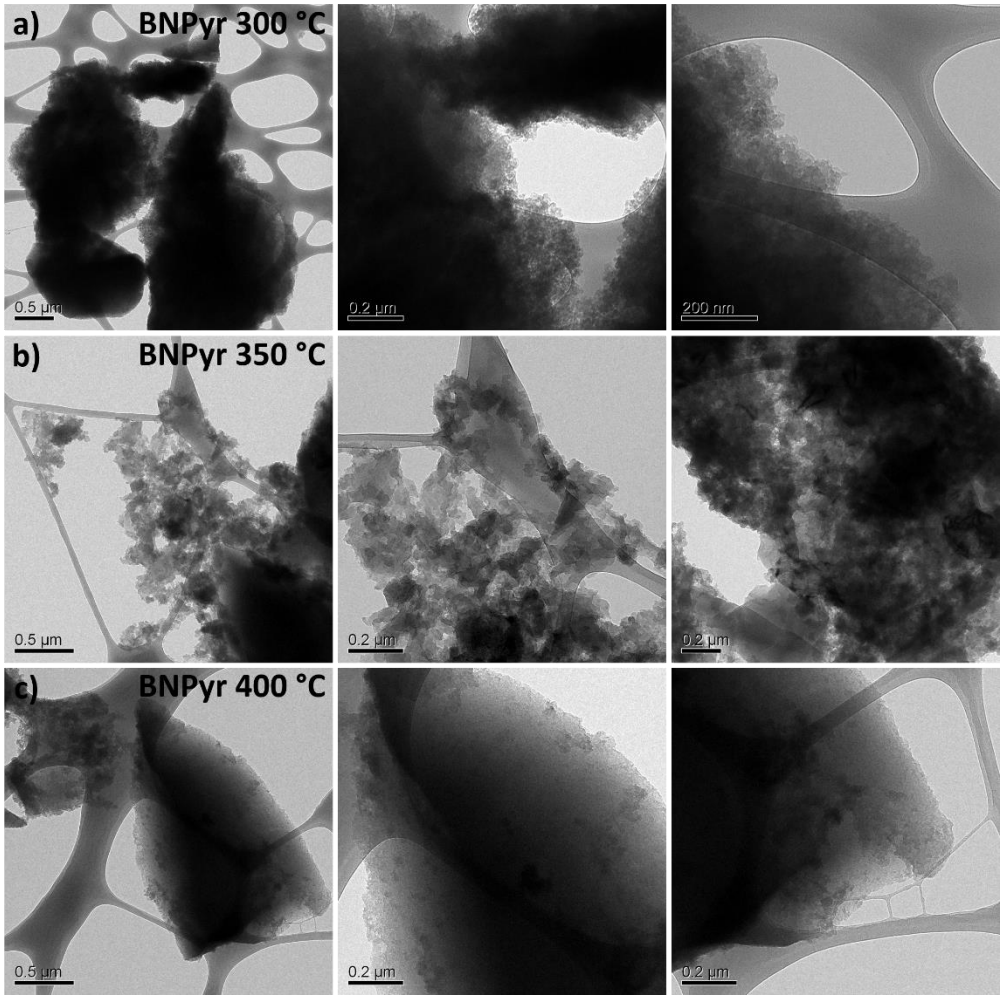

Figure S5. TEM images of a) $BNPyr_{300}$, b) $BNPyr_{350}$, and c) $BNPyr_{400}$.

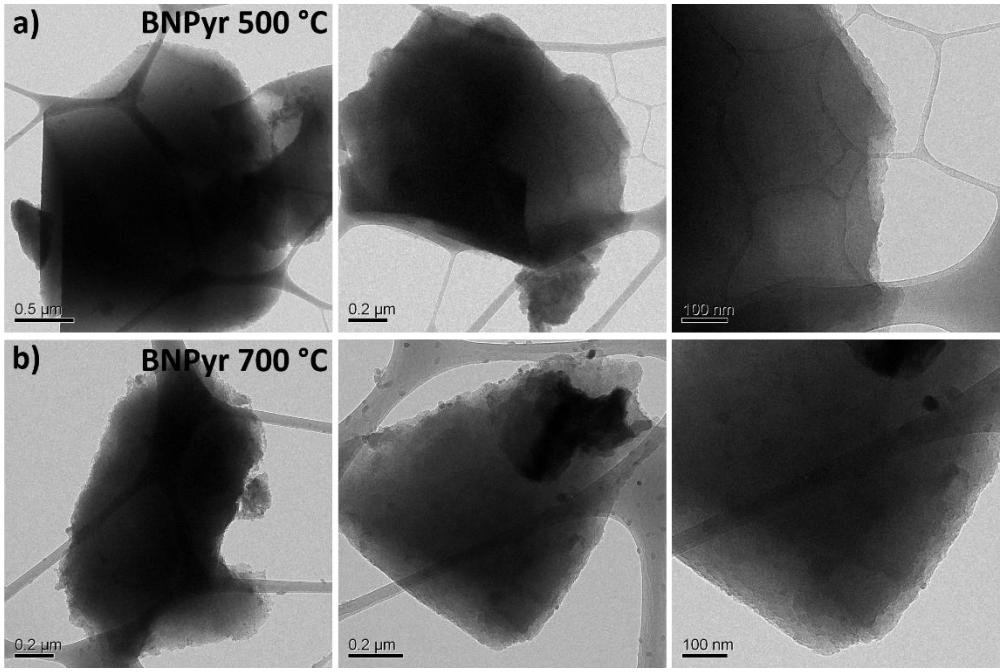

Figure S6. TEM images of a) $BNPyr_{500}$, b) $BNPyr_{700}$.

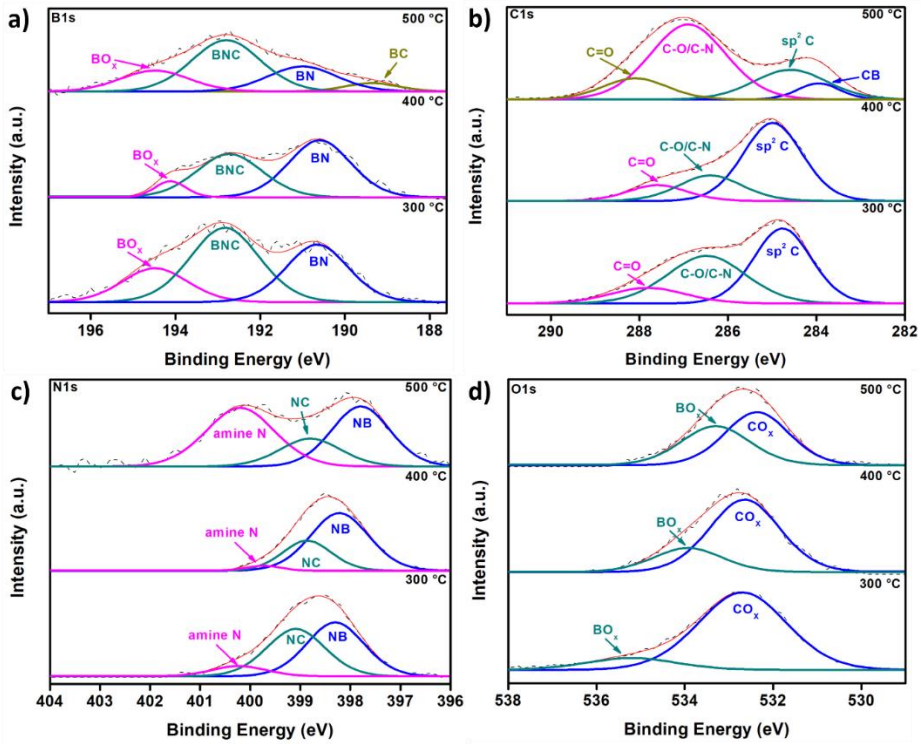

Figure S7. X-ray photoelectron spectroscopy (XPS) characterization. a) C1s, b) B1s, c) N1s, and d) O1s specta of $BNPyr_{300, 400, 500}$. C-B specie can be observed only for $BNPyr_{500}$ as evident by the peaks at ~189.4 eV [1] for B1s and ~283.9 eV [2] for C1s.

Figure S8. Picture of 2 g of $BNPyr_{700}$ made in a single synthesis before grinding.

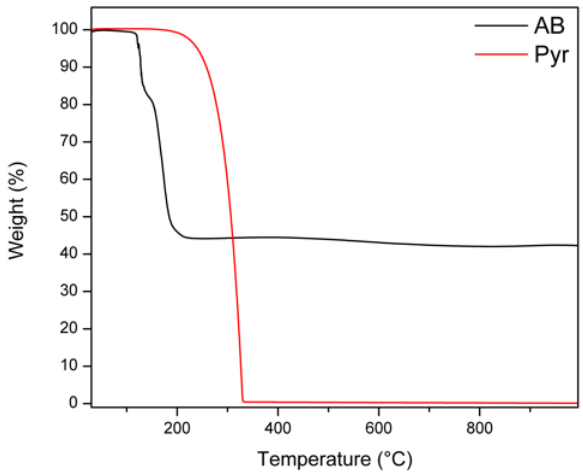

Figure S9. TGA curves of AB and Pyr under N_2 atmosphere.

Figure S10. Powders acquired by pyrolysis of AB at varying temperatures.

Table S1. Elemental analysis and ICP data of BNPyr . AB:Pyr molar ratio was 1:1.

Element	B	N	C	O	H
BNPyr 300 °C	9.43	5.53	78.8	1.52	4.71
BNPyr 350 °C	16.8	14.9	63.5	0.64	4.13
BNPyr 400 °C	21.9	14.9	58.5	0.66	4.01
BNPyr 500 °C	29.9	10.9	49.7	5.54	3.87
BNPyr 700 °C	10.6	12.8	48.9	24.8	2.84

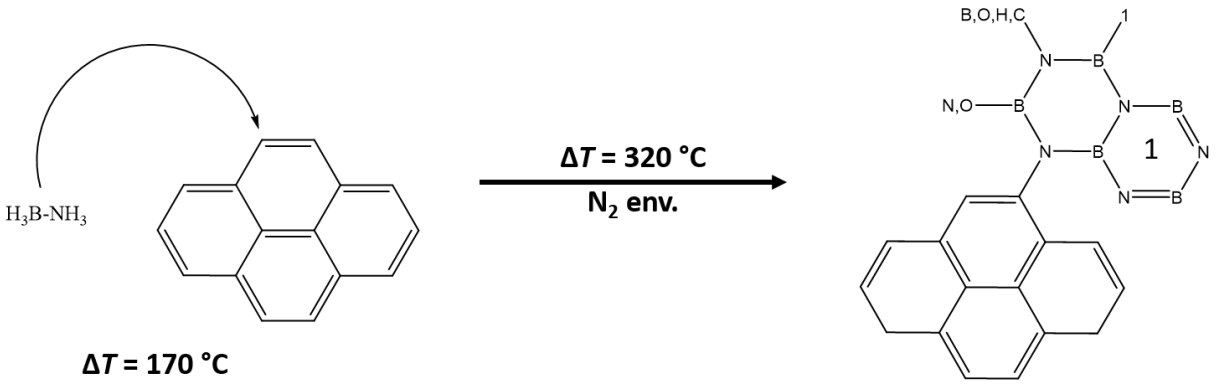

Scheme S1. A proposed reaction mechanism and final structure.
Firstly, the monomers melt when heated to their melting point. Upon reaching 170 °C the AB releases hydrogen and gaseous aminoborane [3] and the AB attacks the pyrene (either through boron or nitrogen atoms) forming a molten intermidiate. Once reaching to 320 °C the molten intermediate starts to condense to form the the structure in Scheme S1.

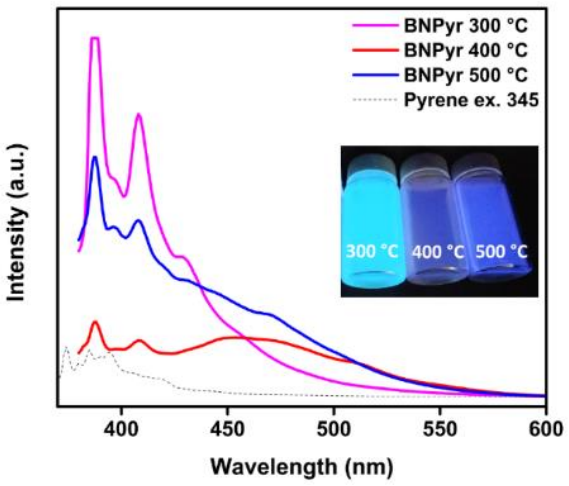

Figure S11. PL spectra of $BNPyr_{300, 400, 500}$, and pyrene in 2-propanol, excited at 365 nm.

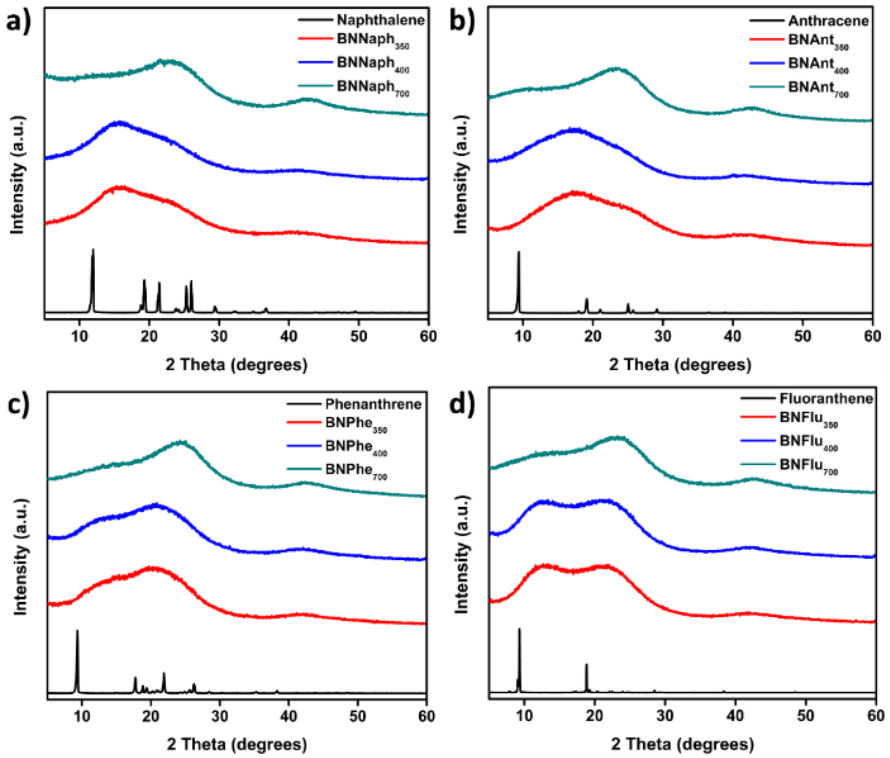

Figure S12. XRD patterns of $BNPAH_{350,\ 400,\ 700}$ using different PAHs. a) BNNaph, b) BNAnt, c) BNPhe, and d) BNFlu.

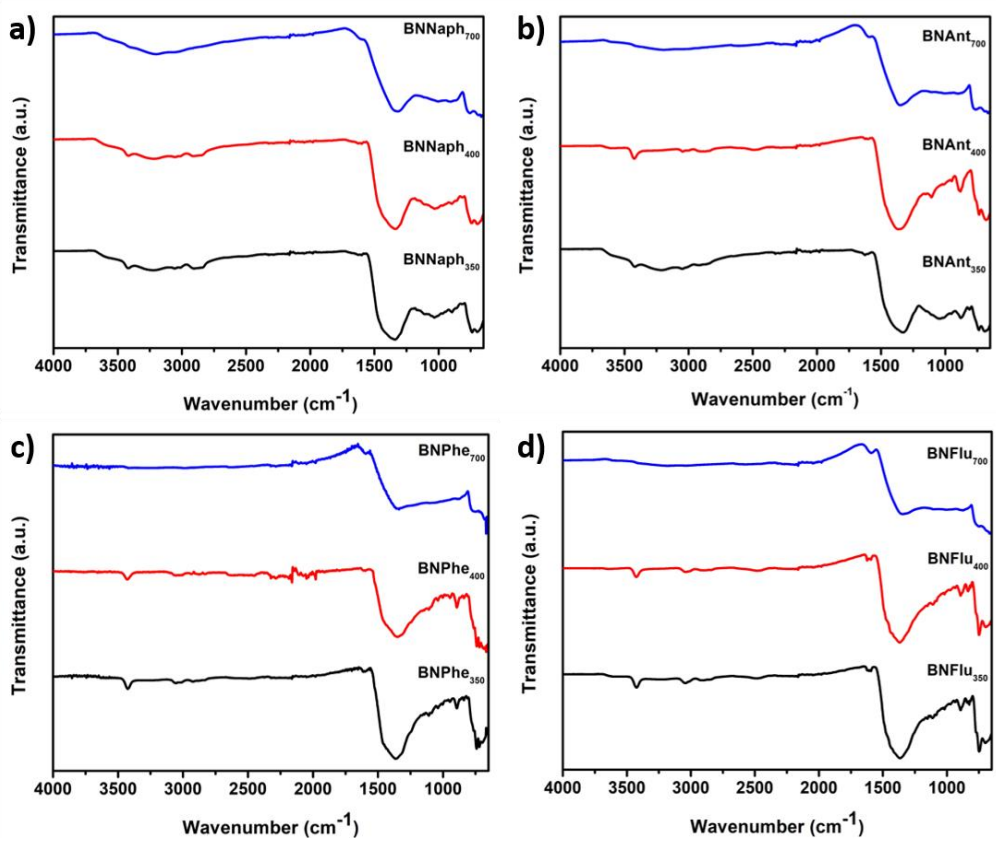

Figure S13. FTIR spectra of $BNPAH_{350,\ 400,\ 700}$ using different PAHs. a) BNNaph, b) BNAnt, c) BNPhe, and d) BNFlu.

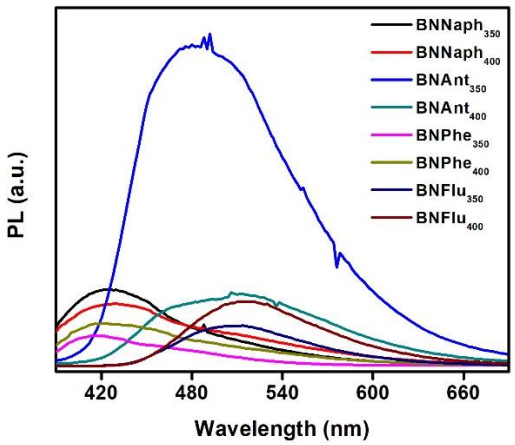

Figure S14. PL (ex. 365) of $BNPAH_{350, 400}$ (Naph, Ant, Phe, and Flu).
These spectra show that for Naph and Ant, there is a quench in the fluorescence as condensation temperature increases probably due to creation of defects. On the other hand, for Phe and Flu, the trend is opposite.

Table S2. EA data for $BNPAH_{700}$

Element	C	N	H
Naphthalene	25.1	19.9	2.42
Anthracene	30.2	19.9	2.58
Phenanthrene	38.7	15.1	3.00
Fluoranthene	41.5	15.8	2.30
Pyrene	48.9	12.4	2.84

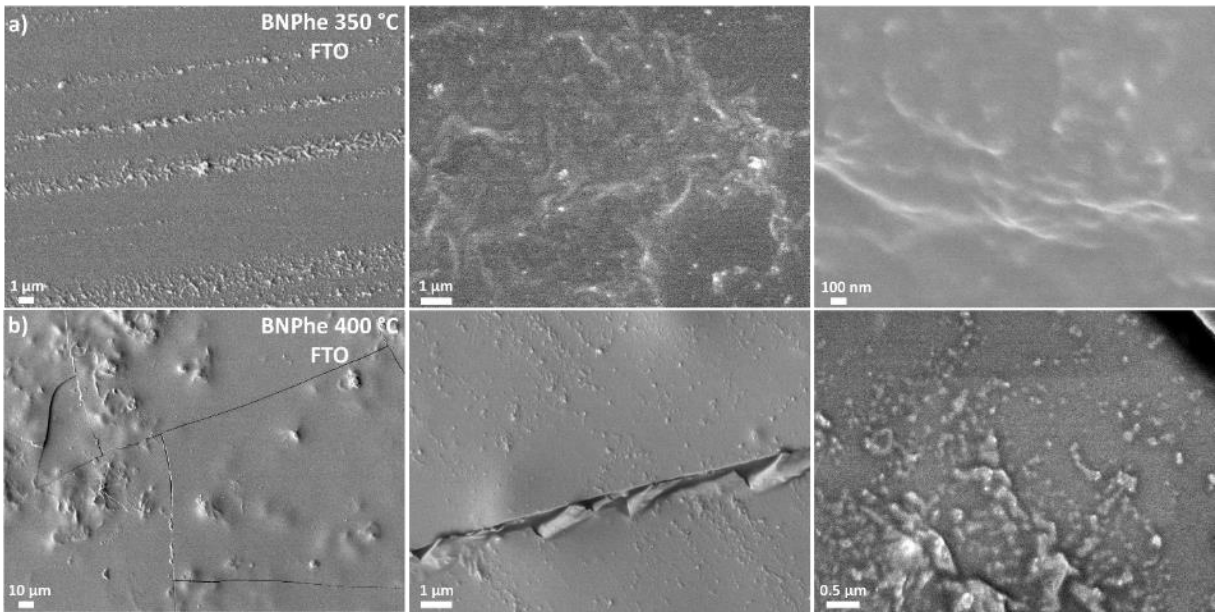

Figure S15. SEM images of BNPhe deposited on FTO. Condensation temperature of a) 350 °C, and b) 400 °C.

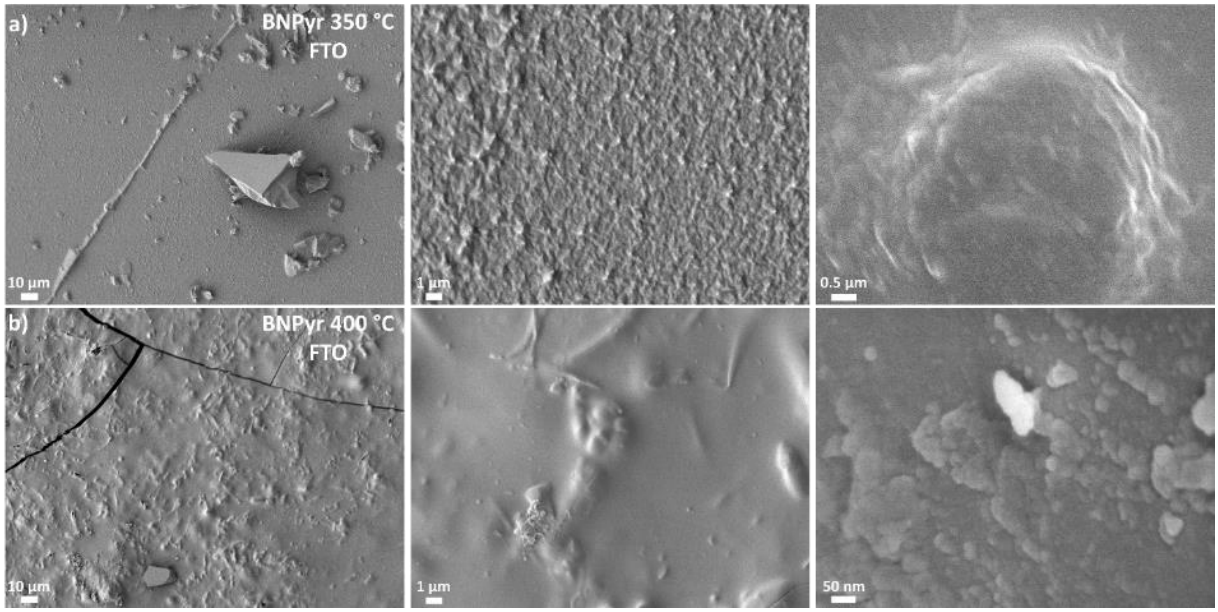

Figure S16. SEM images of BNPyr deposited on FTO. Condensation temperature of a) 350 °C, and b) 400 °C.

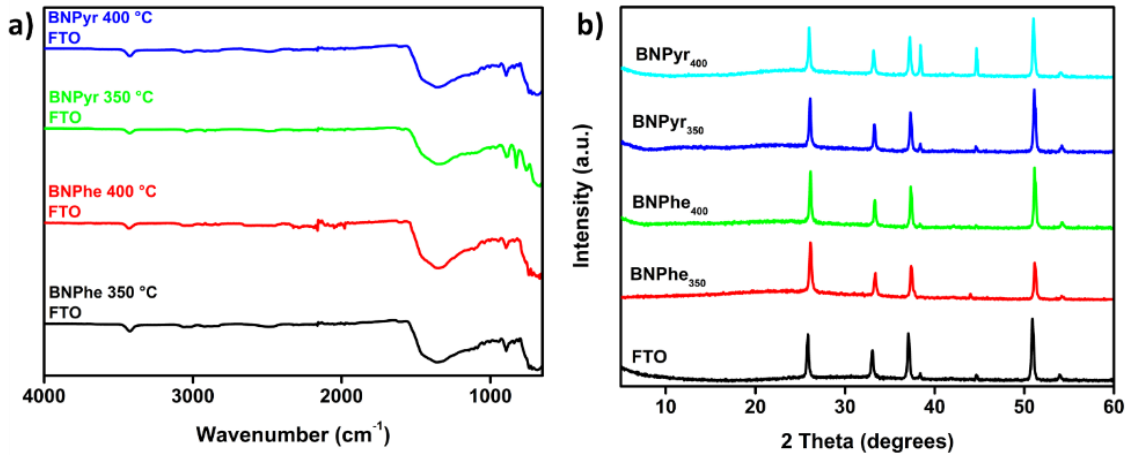

Figure S17. a) FTIR spectra of $BNPyr_{350,\ 400}$ and $BNPhe_{350,\ 400}$ on FTO, and b) XRD patterns of $BNPyr_{350,\ 400}$ and $BNPhe_{350,\ 400}$ on FTO, and a pristine FTO subbstrate.

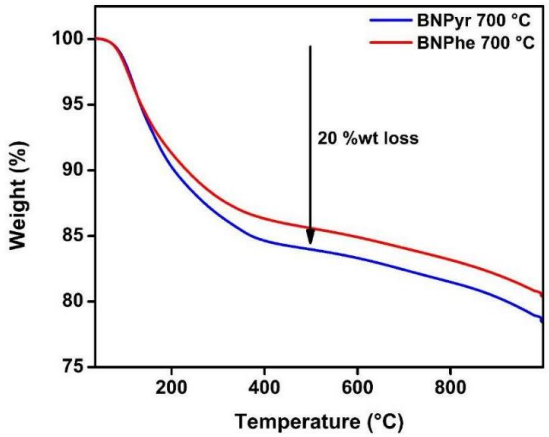

Figure S18. TGA under air of BNPyr, and BNPhe synthesized at 700 °C.

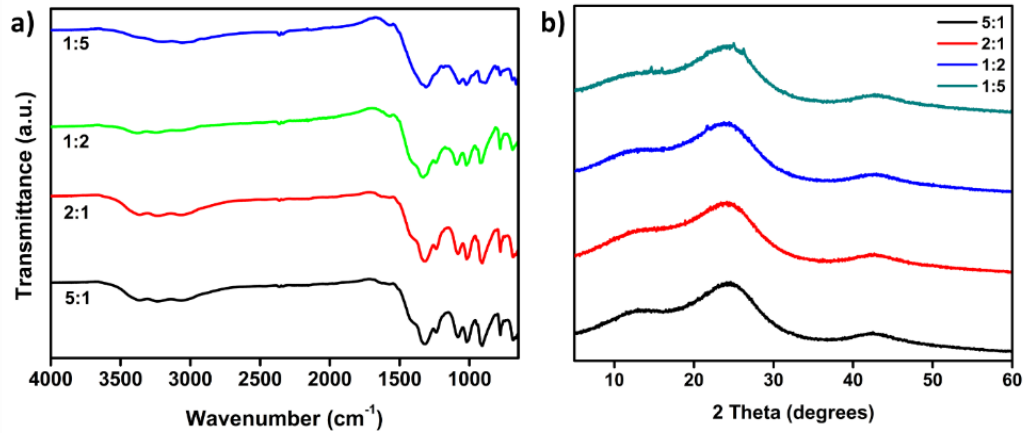

Figure S19. a) FTIR spectra, and b) XRD patterns of BNPyr 700 °C made with AB:Pyr molar ratios.

Table S3. EA and ICP data of BNPyr. X:Y corresponds to AB:Pyr precursor molar ratio.

Element	B	N	C	O	H
BNPyr 700 °C 5:1	11.5	12.4	33.9	39.0	3.18
BNPyr 700 °C 2:1	11.2	12.6	39.9	33.1	3.13
BNPyr 700 °C 1:2	13.7	10.6	46.7	26.4	2.63
BNPyr 700 °C 1:5	16.3	9.33	45.9	26.1	2.31

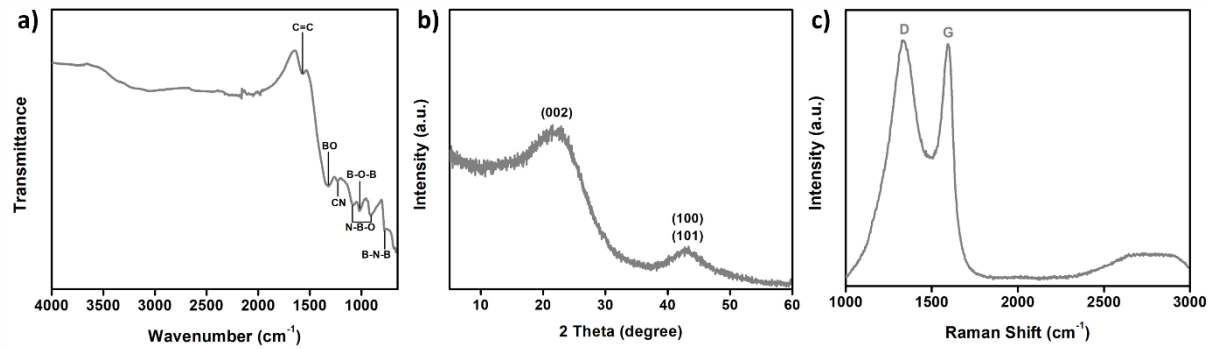

Figure S20. a) FTIR spectrum, b) XRD pattern, and c) Raman spectrum of $BNPyr_{800}$. The ratio between the D and the G band in the Raman spectra (Figure S2, Figure S20) are I_D/I_G=0.81 for $BNPyr_{700}$, and I_D/I_G=1.01 for BNPyr800.

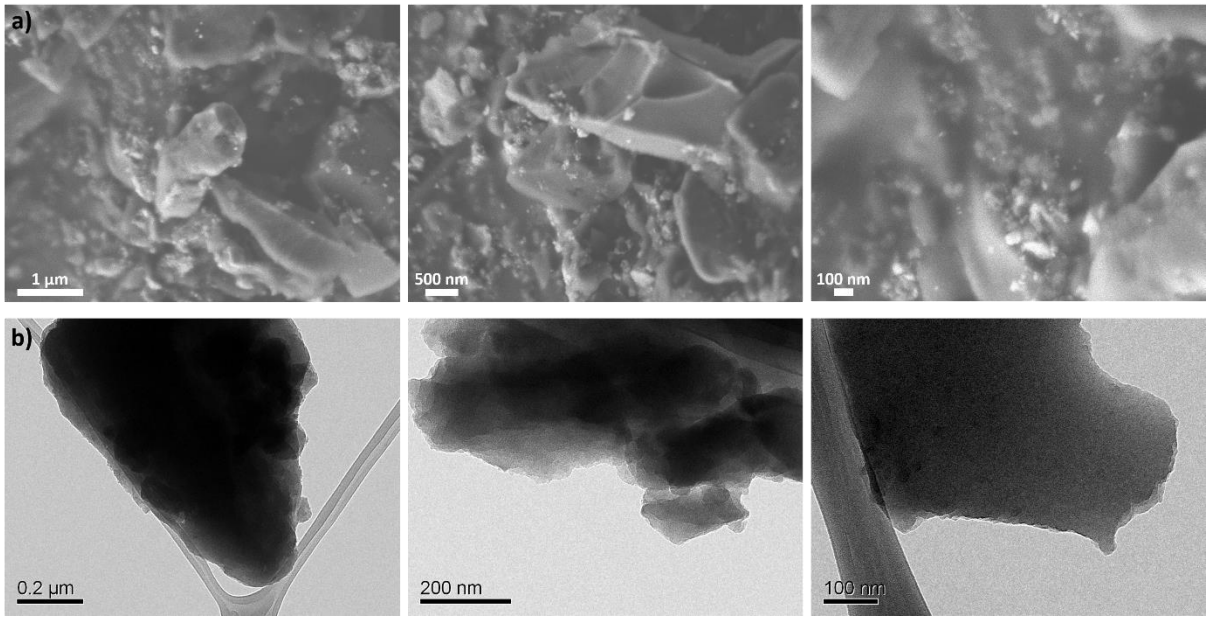

Figure S21. a) SEM, and b) TEM images of $BNPyr_{800}$.

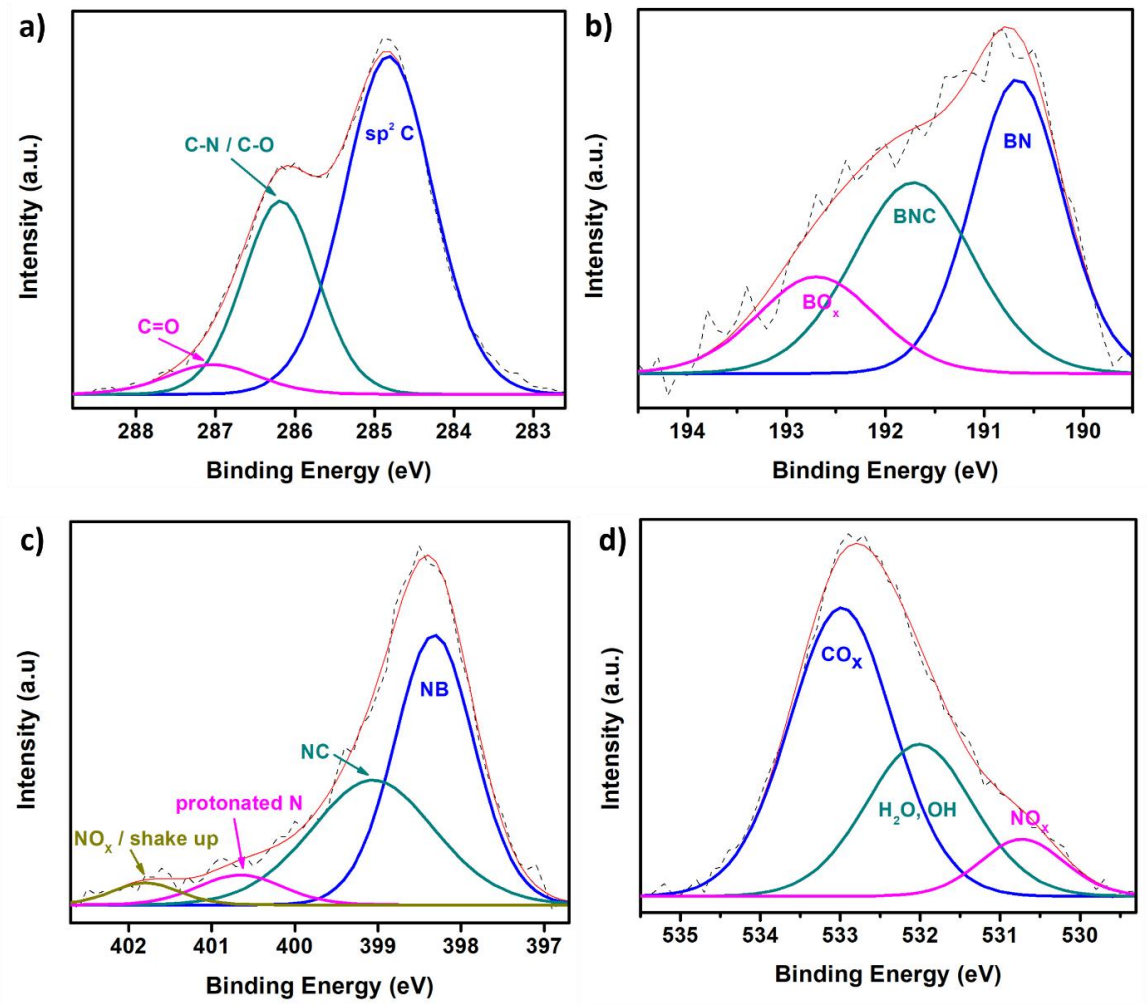

Figure S22. $BNPyr_{800}$ XPS a) C1s, b) B1s, c) N1s, and d) O1s spectra.

Table S4. EA and ICP data of BNPyr 800 °C . AB:Pyr molar ratio was 1:1.

Element	B	N	C	O	H
BNPyr 800 °C	26.6	17.5	49.4	4.46	2.13

Table S5. C/N At. % ratio of $BNPyr_{700}$. X:Y corresponds to AB:Pyr precursor molar ratio.

Element	C/N
BNPyr 700 °C 5:1	3.2
BNPyr 700 °C 1:1	4.5
BNPyr 700 °C 1:5	5.7

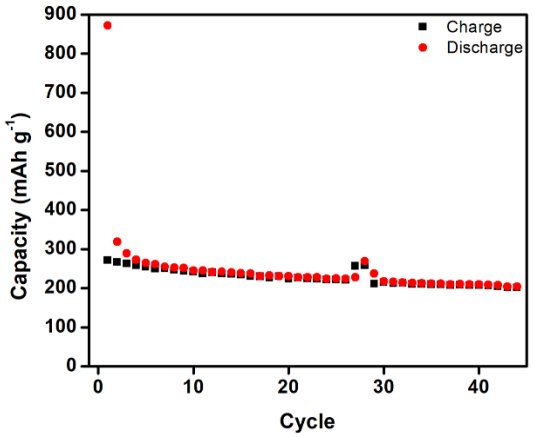

Figure S23. Cycle life stability analysis of $BNPyr_{800}$ 1:1 obtained from polarization under a constant current of 0.1 mA cm^{-2} in a half-cell configuration vs. Li metal.

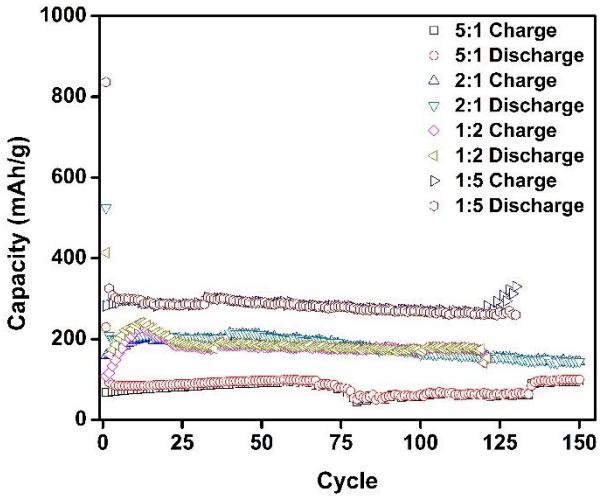

Figure S24. Charge-discharge curves of capacity *vs* cycle number of BNPyr synthesized at 700 °C and a molar ratio of AB:Pyr.

Supporting Information Refrences

[1] M. Favaro, F. Carraro, M. Cattelan, L. Colazzo, C. Durante, M. Sambi, A. Gennaro, S. Agnoli, G. Granozzi, *J. Mater. Chem. A* **2015**, *3*, 14334–14347.

[2] H. Fang, C. Yu, T. Ma, J. Qiu, *Chem. Commun.* **2014**, *50*, 3328–3330.

[3] S. Frueh, R. Kellett, C. Mallery, T. Molter, W. S. Willis, C. King, S. L. Suib, *Inorg. Chem.* **2011**, *50*, 783–792.